Research Article

Panoramic Image Generation Technology for Full Digital Stereo 3D Reconstruction in Water Conservancy Surveying and Mapping Engineering

Fangfang Mao[1] and Lei Zhao [2]

[1]*Department of Civil Engineering, Zhengzhou Shengda University, Zhengzhou 451192, China*
[2]*Henan Electric Power Survey and Design Institute Co. Ltd, Power China Group, Zhengzhou 450000, China*

Correspondence should be addressed to Lei Zhao; 1817300037@e.gzhu.edu.cn

Due to the lack of image feature extraction in traditional panoramic image generation technology, the effect of 3D reconstruction of physical objects is poor. In this paper, fully digital stereoscopic 3D reconstruction technology is introduced in water conservancy surveying and mapping engineering to ensure complete panoramic image generation. Through in-depth analysis of the principle of 3D reconstruction technology and the database, the detailed water conservancy surveying and mapping engineering images are obtained, the feature vectors of the obtained panoramic images are matched, and the database is compared and positioned according to the matched position features. By using the initial position camera and calibration features, comparison and query are conducted with the image database, to remove the worthless confidence data, retain the outline of the object with reference value, obtain a fixed pose center point, and remove the overlapping area in the process of 3D reconstruction after calculating the outline of the image. Finally, the automatic generation of panoramic images is realized. Finally, the results of experimental analysis show that the panoramic image generation technology of the fully digital stereoscopic 3D reconstruction proposed in this paper has a relative accuracy of 49% compared with the traditional image generation method, and the effect of image generation is relatively good, which has a certain use value.

1. Introduction

When carrying out a water conservancy project, they need to carry out engineering surveying and mapping for each of their procedures during the project initiation, design, and completion acceptance. Therefore, the problem that plagues water conservancy project surveyors is the work efficiency of water conservancy projects [1–3]. Now there is a new topographic survey, which is fully digital stereo 3D reconstruction. This new breakthrough is a breakthrough after GPS technology. The technology of fully digital 3D reconstruction has been recognized and promoted in 3D models [4–6]. Because there is currently no system that supports fully digital stereo 3D reconstruction, detection, and mapping, the current use of fully digital stereo 3D reconstruction is to switch and combine multiple systems to assist in completing the task, which hinders the surveying and mapping work and reduces work efficiency. The adoption of fully digital stereo 3D reconstruction digital stereo in hydraulic engineering surveying and mapping has brought difficulties.

Overlapping image points can regenerate panoramas in the order of image matching, image projection, and image combining. Under normal circumstances, the image matching method is used. By randomly extracting a range, an image is locked in this range, indicating that the center of this range is the relative position of the original center [7–9]. It can be expressed in a similar way. The combination of multiple pictures is used to form a panoramic image, and some photos may be repeated. For the recombination of the images formed in this situation to form a new panoramic

image, shooting technology shall be necessary. The photographer uses the reflex of one lens to take pictures and shoots in multiple directions through wide-angle and fisheye lenses. A panorama photo is formed by taking general-purpose software. When generating a new panoramic photo, Silverlight, Flash, and other software shall be used to combine and switch. The formation and aging of the image is mainly based on the structure of the image software, and the processing operation of the image is based on the real shooting environment and shooting technology. Traditional technology is adopted for synthesis to reduce the accuracy of the image, resulting in a gap between the data inside and outside the camera [10–12].

The goal of this paper is to study the way of information extraction in the fully digital stereo 3D reconstruction technology in the special environment of Guizhou Province. By dealing with this situation, the fully digital 3D reconstruction technology can be better applied to water conservancy projects, and it can be seen that this breakthrough brings prospects and even promotes social and economic development.

2. Methods

2.1. Fully Digital Stereo 3D Reconstruction Technology. In order to shorten the construction period of water conservancy projects as much as possible, avoid packet loss of data related to water conservancy project design during transmission, or data information asymmetry due to time delay, the overall architecture of water conservancy projects can be topologically configured [13]. This paper takes the database collected in the actual use of the water conservancy project as the basis of the research, and uses the fully digital stereo 3D reconstruction technology to perform 3D reconstruction based on the dynamically captured images of the water conservancy project in real time. Meanwhile, after the 3D data of the water conservancy project is dynamically acquired, it needs to be processed and balanced in a unified manner, compared with the topographic structure characteristics of the Fenix water conservancy project, and using its more complex features, the data information that appears can be matched with the structure of the address surface, and the data information indicated by the topography can be fully used, as shown in Figure 1. Taking advantage of the different environments of $Z1$, $Z2$, and $Z3$, there is no relevant data in I in the borehole according to $Z3$, which leads to the replacement of the first layer of data when the second layer of data is collected. Through the data collection in the final process, it is necessary to use a difficult interpolation method, and it is also necessary to interpolate the values between the first layer and the second layer. After the interpolation is completed, the interpolation is used according to the height difference between the first layer and the second layer to figure out the data of the second layer.

According to the rules of the above figure, the calculation can be performed in this way, and the boundary contours can be connected with different layers, and a new address model can be generated from this. Compared with the previous calculation methods with different frequencies, this fully digital calculation method is faster through the filtering
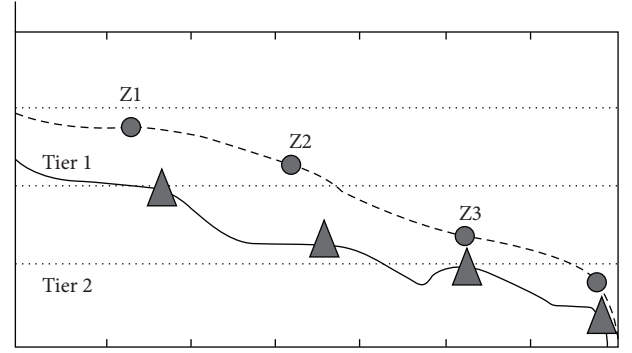

FIGURE 1: Cointerpolation through borehole and surface data.

calculation of the basic prediction method, and is more widely used in water conservancy projects [14]. The formula of the input data is represented as follows:

$$x(t) = \sum_{n=1}^{M} U_n \sin\left(n2\pi f_0 t + n2\pi\Delta f t + \theta_n\right) + U_0. \qquad (1)$$

In the above formula, n represents the harmonic order, and if $n = 1$, which represents the fundamental component. f_0 represents the fundamental frequency; Δf represents the starting number of any first harmonic of the frequency offset data system; and U_0 represents the amplitude generated after the nth harmonic of the DC component.

If only the fundamental wave component is analyzed and $\theta(t) = 2\pi\Delta f t + \theta_1$, then

$$\frac{d\theta(t)}{dt} = 2\pi\Delta f. \qquad (2)$$

Let the discrete difference equation replace expression (2), when the period of the time step is $T_0 = 1/f_0$.

$$\begin{aligned} \Delta\theta &= 2\pi\Delta f \Delta t \\ &= 2\pi\Delta f T_0 \\ &= \frac{2\pi\Delta f}{f_0}, \\ f &= f_0 + \Delta f \\ &= f_0 + \frac{f_0 \Delta\theta}{2\pi}. \end{aligned} \qquad (3)$$

Equation (3) calculates the frequency measurement formula. The ideal frequency of the fundamental wave satisfies $f_0 = 100$ Hz, and the real frequency normally fluctuates slowly around f_0, so the phase deviation needs to be calculated correctly. Calculate the actual frequency f.

The real and virtual values that can be obtained through the principle of fully digital stereo 3D reconstruction are

$$\begin{aligned} a_n &= \frac{2}{N} \sum_{k=0}^{N-1} x(k)\cos\left(nk\frac{2\pi}{N}\right), \\ b_n &= \frac{2}{N} \sum_{k=0}^{N-1} x(k)\sin\left(nk\frac{2\pi}{N}\right). \end{aligned} \qquad (4)$$

In the formula, N is the number of periodic sampling points and $X(k)$ is the sample data sequence.

The initial phase angles θ_n of the fundamental wave and each harmonic are

$$\theta_n = \arctan\left(\frac{b_n}{a_n}\right). \tag{5}$$

Figure 1 shows that when the sample chip AD7606 sets the fixed sample frequency $f_s = 400$ Hz, N is

$$N = \frac{f_s}{f}. \tag{6}$$

If $f = f_0 = 100$ Hz, N is an integer:

$$\begin{aligned} N &= \frac{f_s}{f} \\ &= 80. \end{aligned} \tag{7}$$

When $f \neq 100$ Hz, N is a real number most of the time. Spectral leakage occurs because the sampling frequency does not match the actual measurement frequency in a true sense [15, 16]. However, the premise is that the number of sampling points in the period is an integer to reduce the problem of spectral leakage, and the fundamental wave component will occur. The improved formulas are (8) and (9)as shown as follows:

$$a = \frac{2}{N_1} \sum_{k=0}^{N_1-1} x(k)\cos\left(k\frac{2\pi}{N_2}\right), \tag{8}$$

$$b = \frac{2}{N_1} \sum_{k=0}^{N_1-1} x(k)\sin\left(k\frac{2\pi}{N_2}\right). \tag{9}$$

When affirming N_1, the idea of N_2 is as follows.

(1) It is known by formula expression that N is an integer, rounded up to:

$$N_1 = \text{round}\left(\frac{f_s}{f}\right). \tag{10}$$

In the formula, round () is the function of rounding calculation.

(2) The number of sample points N is converted, and the corresponding Fourier coefficients $\cos 2k\pi/N$ and $\sin(2k\pi/N)$ change accordingly, and the amount of N change is as follows:

$$\begin{aligned} \Delta N &= N_1 - N \\ &= N_1 - \frac{f_s}{f}. \end{aligned} \tag{11}$$

Then the N in Fourier factors $\cos(2k\pi/N)$ and $\sin(2k\pi/N)$ should be corrected to

$$\begin{aligned} N_2 &= N_1 + \Delta N \\ &= 2N_1 - \frac{f_s}{f}. \end{aligned} \tag{12}$$

Previously, three-dimensional reconstruction was performed by expressing the initial gap between the two cycles before and after the two data cycles, which extended the tracking time. According to the data with a frequency of 100 Hz, assuming that the period is 45 ms, the value of f_s is set to 900 Hz; when the data value of the period is 160, the period is 4 ms, and 16 data values can be calculated. The degree of two cycles is 4π, so 0.2 cycles is a constant number [17]. Therefore, θ is taken as a reference number according to T to be 0.4π.

When the difference between the start points of the period T_2 and the start point in the time end is 16 values, it is fixed, so the formula for the phase angle difference is represented as follows:

$$\begin{aligned} \theta_{T_{21}} &= \theta_{T_2} - \theta_{T_1} \\ &= \arctan\frac{b_{T_2}}{a_{T_2}} - \arctan\frac{b_{T_1}}{a_{T_1}}. \end{aligned} \tag{13}$$

Therefore, points P_2 and P_1 have different values, so $\Delta\theta = \theta_{T_{21}} - \theta_T$ cannot be used. The $\Delta\theta$ solution process is as follows:

$$\begin{aligned} \Delta\theta &= \theta_{T_{21}} + 2\pi, \\ \Delta\theta &= \text{mod}(\Delta\theta, 2\pi), \\ \Delta\theta &= \Delta\theta - \theta_T. \end{aligned} \tag{14}$$

In the above formula, $\text{mod}(\Delta\theta, 2\pi)$ is the remainder of $\Delta\theta$ to 2π.

Therefore, the calculation formula of the actual frequency f is

$$\begin{aligned} f &= f_0 + \Delta f \\ &= f_0 + f_0\left(\frac{\Delta\theta}{\theta_T}\right). \end{aligned} \tag{15}$$

However, the real f is not 100 Hz, they are fluctuating around 100 Hz. When $f \neq 100$ Hz, the value of f needs to be obtained through multiple calculations.

2.2. Panoramic Image Generation for Water Conservancy Surveying and Mapping. Panoramic images have many advantages in application, such as more realism and faster filming time, and the situation in the field is not held back by the situation of the drawing. Before the image is formed, the photographer needs to take a two-dimensional photograph of a three-dimensional object, and hide some features of the geometric image due to the illumination. Using the model of the camera to fix the map, through the original data background, and using the formed three-dimensional picture coordinate data, the construction of the three-dimensional image is completed.

Principles of 3D reconstruction technology: The construction of 3D images is by the way of combining the geometric features of multiple images, which is widely recommended in the market. If only one camera is used, there will be an inability to correctly find the specific position

and direction in the camera. If the cameras of other addresses are used to work together, they can shoot at one time and one space, which is called the imaging point of the second camera [18]. At the same time, the specific position of the space can be quickly determined to complete the panoramic image work.

Image information acquisition: The so-called GPRS is to process, analyze, and manage the Beidou satellites and the collected data. Therefore, the early warning software of 3D hydraulic engineering is established. In the case of high-level maps and geological information, for the three-dimensional surface model and geological model, the visualization of the location can be realized by managing and searching through the data provided by the WGD80 coordinate software [19].

The combination of monitoring system and three-dimensional system is realized through the geodetic coordinate system. Through the geodetic coordinate system, the collected equipment is substituted into the three-dimensional dynamic system, and the 3D model is realized by the fusion of measuring instruments and information data. The so-called data collection is a data system that analyzes geology, geological design, informatization, and stability, and needs to be supported by other data analysis.

The system is divided into two modules.

2.2.1. Formation and Analysis of Geological Information

(i) The three-dimensional model of the address formed by using the surface information and borehole information.

(ii) Through the coordinate system of the monitoring system, monitoring equipment is added to the three-dimensional data dynamic monitoring platform.

(iii) Using geological sliding edge to distinguish address zone

(iv) Add the address section line to the basic system, connect the relative sections of the address section line, and use the section line to analyze after the connection to obtain the relevant geological section diagram.

(v) Analyze the monitoring platform information, that is, perform hierarchical analysis on the monitoring information.

(vi) Give data analysis capabilities, including cross section analysis. Information about that place can be obtained by simply clicking the mouse or entering a location.

2.2.2. Obtain Data Analysis and Alarms

(i) The communication equipment such as Beidou satellites or GPS functions are used to analyze the information received, and feeding back the collected information to the background.

(ii) The serial number of the monitoring system or the relevant information transmitted to Oracle by the Big Dipper and GPRS is connected, and the user can monitor the device by clicking the mouse.

(iii) Collect device information by clicking the mouse, determine the collected data, and build the model by collecting the time sequence of alarm APMA.

The relevant information of the picture can be obtained by managing the data in the camera before receiving the picture. When the information is obtained, the result of overlapping the left 1 and right 1 image is presented at point t_1. For the level of system angle rotation, the image results of overlapping left 2 and right 2 are presented at point t_2, and the collected images are differentiated and managed correspondingly, and then the image files are reconstructed.

2.3. Camera Coordinate Positioning and Pose Parameter Setting.

When the camera is used to measure the panorama, its azimuth coordinates are accurately determined, and the camera can change the azimuth with the instrument. When the camera is aimed at the panoramic object measurement, there will be four coordinate information, using the right-hand coordinate method, as shown in Figure 2.

It can be seen from Figure 2 above that the coordinate system is the global coordinate system. Using the three-dimensional positioning of the global scene, the three-dimensional coordinate information is informed in this scene, and the accurate positioning of the instrument can be carried out. The coordinates of the instrument are $O_2 - a_2b_2c_2O_1 - a_1b_1c_1$, where the abscissa is the horizontal data representing the zero-degree direction of the instrument. Through the information in the zero-degree direction, the spatial dynamics of the instrument can be determined. Secondly, the coordinates of the camera are $O_5 - a_5b_5c_5$ data centered on the left side, and can be operated according to the tilt angle of the horizontal axis as the center. According to the coordinate system with the center of the camera as the origin, the position of the camera changes according to the direction of the coordinate system, and the camera changes with the coordinate changes of the instrument $O_3 - a_3b_3c_3$.

Using the original coordinate data of the camera and the azimuth method of the instrument, the coordinates of the camera are fixed with the original data to prevent deviation.

The horizontal degree of the meter in the original data is $0°$ and the vertical angle is $90°$. This data can infer the rotation direction of the camera's coordinate system and the coordinate system of the meter. Set the coordinate rotation of the camera in the coordinate system to W, and convert it by formula. Assuming that the camera coordinates and the instrument coordinate rotation are W, the following formulas need to be satisfied:

$$F = WO_{3D}. \tag{16}$$

In the above formula, O3D represents the spatial 3D coordinate data. The coordinate data representation of the camera is determined by using the meter data (A_1, B_1) to be (A_2, B_2). The formula for calculating the spatial coordinate point through the coordinate data of the camera and the meter is shown in the following formula (17). At the same
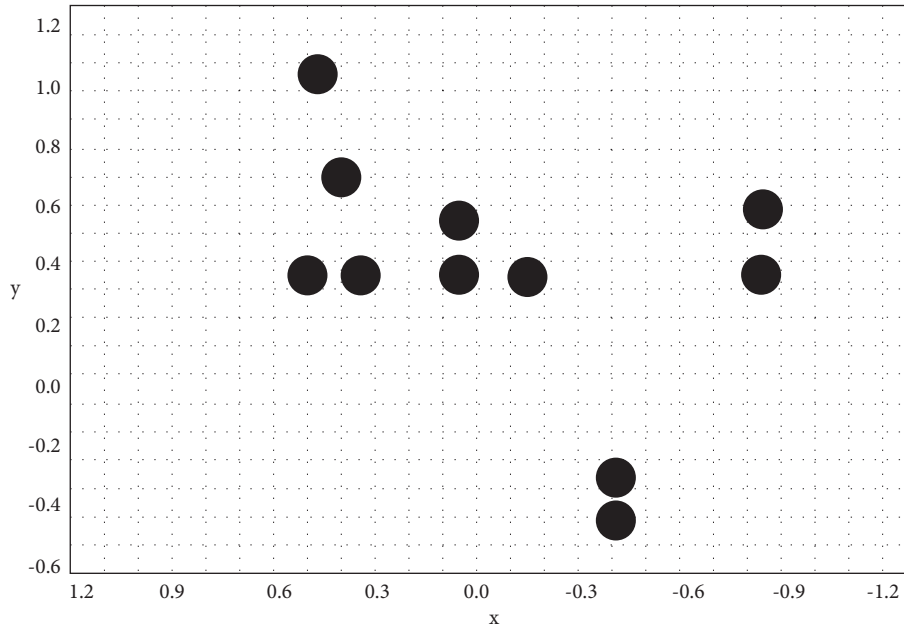
Figure 2: Coordinate positioning.

time, the spatial coordinate system also requires the camera and instrument coordinates to satisfy the formula at the same time.

$$T = (A_1, B_1) C_1 + (A_2, B_2) C_2. \tag{17}$$

In the above formula, the coordinates of the camera and the coordinates of the meter are represented by C_1 and C_2, respectively. Calculate the coordinate data through the coordinates constructed above.

Extraction of Center Point Coordinate: Many special shape points are obtained from the space coordinate axis. We usually choose circles as the research target. Figure 3 shows the obtained coordinate point image.

As shown in the figure above, the fixed image contains many marker points. The manual operation method is used to collect and process the edge distribution of some images evenly.

The typical sign point of the sign image in Figure 4 will be in an ellipse state in the camera, and the special information in the camera is identified through a circular tree shape.

The circularity value is

$$Z = 4\pi \cdot \frac{S}{L^2}. \tag{18}$$

In formula (18), the value of circularity is represented by Z. The contour length of the image is denoted by S. The contour area is denoted by L. When approaching a circle during the contour reconstruction, the metric value is close to 1, if the metric value is not less than 1.

Because the range of circularity value is not affected by nonellipse data, and by the range of length, the interference

of circular data can be reduced. If the selected length value is in the range of $L_{\min} < L < L_{\max}$, its characteristics should be preserved. The punctuation map that can be obtained is shown in Figure 4.

Through the line drawing data, the positioning relationship between the coordinate center and the image is determined, so that the center of the coordinate circle coordinate is more integrated. Through the extraction of the outline of the marker points, each marker point is connected, as shown in the center connection line diagram shown in Figure 5.

Image Reconstruction: The coordinates $O_1 - a_1b_1c_1$ and the camera coordinates $O_5 - a_5b_5c_5$ obtained from the data measured by the above camera coordinates are connected with the image outline in the instrument coordinates $O_1 - a_1b_1c_1$ and the image of the coordinate system $O_5 - a_5b_5c_5$, and the data conversion is performed in an overlapping manner, and the numbers in $O_5 - a_5b_5c_5$ are converted into $O_1 - a_1b_1c_1$. The formula is shown as follows:

$$\begin{bmatrix} a \\ b \\ c \end{bmatrix}^n = \begin{bmatrix} x_{11} & x_{12} & x_{13} \\ x_{21} & x_{22} & x_{23} \\ x_{31} & x_{32} & x_{33} \end{bmatrix} \begin{bmatrix} a_0 \\ b_0 \\ c_0 \end{bmatrix}^n + \begin{bmatrix} x_{41} \\ x_{42} \\ x_{43} \end{bmatrix}^n$$
$$= W \begin{bmatrix} a_0 \\ b_0 \\ c \end{bmatrix} + M. \tag{19}$$

In formula (19), W is the rotation matrix and M is the translation matrix. Converting all the image information features in $O_5 - a_5b_5c_5$ in the coordinate system into the coordinate system $O_1 - a_1b_1c_1$, the automatic generation of three-dimensional reconstruction of panoramic images can be realized.

Using the characteristics of black and white properties, high brightness, and strong directionality of fully digital stereo 3D reconstruction, and using lasers as the measurement technology for the distance between the two, it has the characteristics of achieving measurement accuracy and measurement efficiency, and easy to operate [20]. With the development of science and technology, three-dimensional reconstruction technology, computer technology, and sensor technology have also been advanced development, especially the accuracy of panoramic image generation, work efficiency, interference, and distance measurement, etc., have been significantly improved. The panoramic image generation function module is also increasing, and its application fields are gradually expanding.

Panoramic image generation can be roughly divided into triangular panoramic image generation, phase panoramic image generation, and impulse panoramic image generation according to the image generation method. The measurement range of triangular panoramic image generation and phase panoramic image generation is small, so the measurement range is 0.5 m~100 m, while the measurement range of pulsed panoramic image generation is large up to
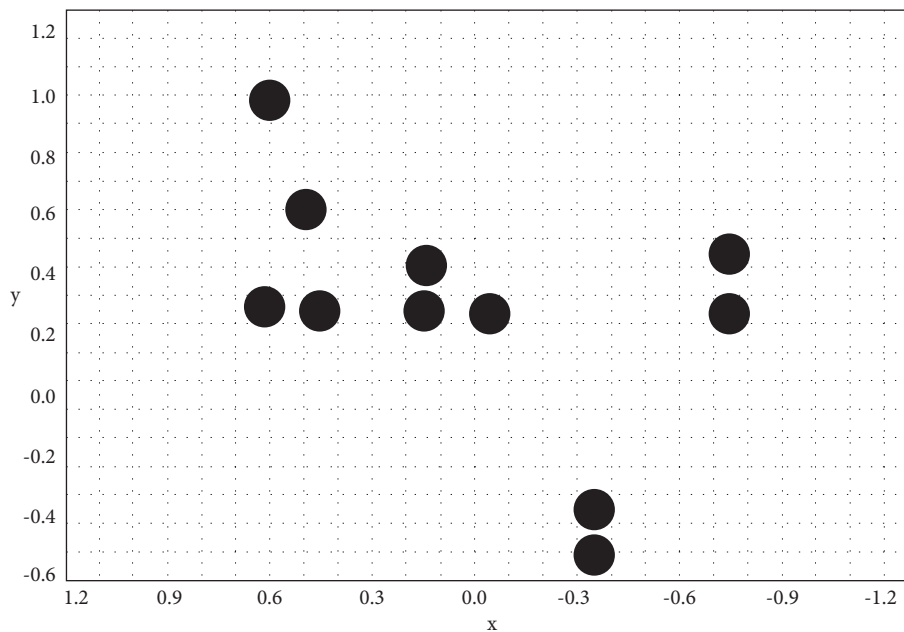
FIGURE 3: Calibration image.

FIGURE 4: Marking point outline.

l m~6000 m. Therefore, due to the special needs of topographic surveying in water conservancy projects, pulsed panoramic image generation is used.

The pulse panoramic image generation method mainly uses noncontact high-speed lasers to complete the rendering of topography and landforms, and at the same time uses the point cloud method to extract the surface features of the object. The way to take pictures of the object is to use a laser generator to emit class I laser pulses, and the receiver receives the laser pulses reflected from the surface of the measured object. When measuring the distance between the measured object and the 3D laser instrument, the vertical angle and horizontal angle of the built-in angle measurement system can be used to generate X, Y, Z coordinate values corresponding to different scanning points in the coordinate system according to the panoramic image. The 3D laser scanner records the 3D coordinates of the laser point and records the reflection intensity value of the measured object; the measurement principle of pulsed panoramic image generation is shown in Figure 6.
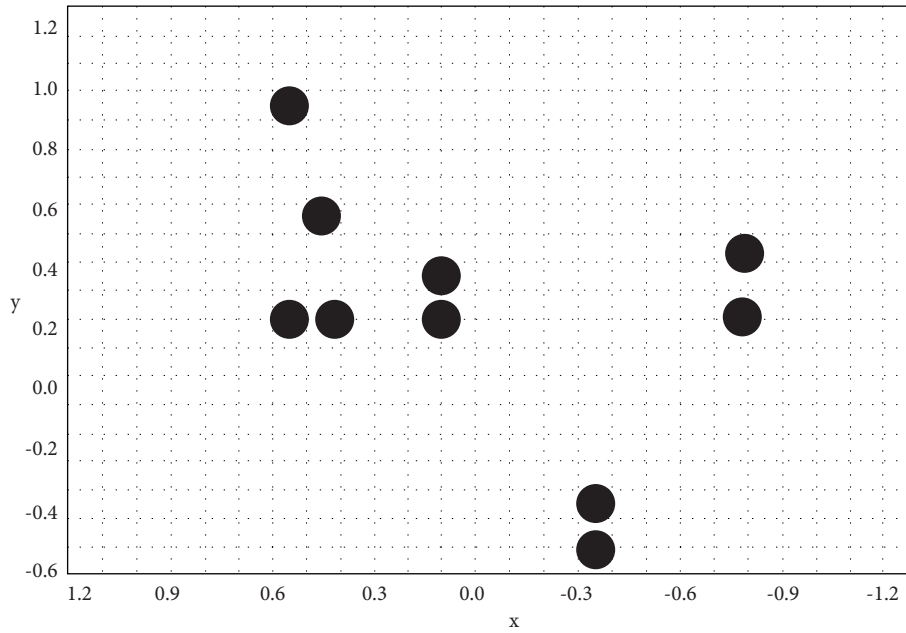
Figure 5: Center point connection diagram.
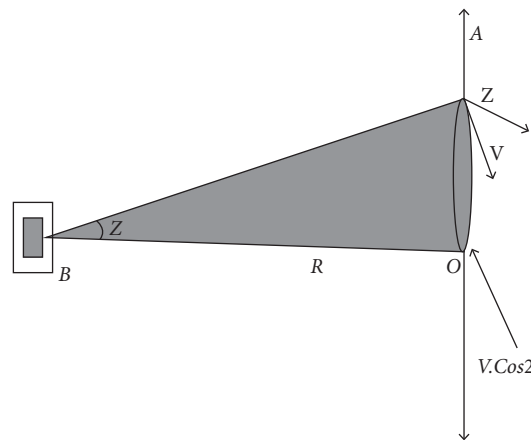
Figure 6: Measurement principle diagram of pulsed panoramic image generation.

2.4. Experimental Results and Analysis. In order to effectively test the practicability and effectiveness of the panoramic image automatic generation technology constructed by the fully digital stereoscopic 3D technology, the following experiments will be carried out. The size of the image used is 2000×1500. A 3D image platform is built under the operating environment of Windows 8. A camera with a resolution of $640 \, \text{pi} \times 520 \, \text{pi}$ is used to obtain a panoramic 30-frame image of a park for experimental research samples. The original image selected in this paper is shown in Figure 7.

(1) Selection of erection stations for water conservancy projects. In the measurement process of water conservancy projects, it is necessary to obtain real-time data information in combination with the actual project, and in the process of erecting water conservancy projects, it is necessary to measure for

auxiliary basis. After completing the actual engineering measurement, the water conservancy project can select the number of erection stations according to the previous E level.

(2) Geographic survey. The scanner needs to be measured. The principle of the scanner in the engineering application process is to use the spatial coordinate data for the coordinates corresponding to the transmitter. Therefore, the data needs to be unified. In the operation records used, it is necessary to calculate the data between the two parallel distances according to the measured data and coordinate coefficients. At the same time, RISCANPR 0 software can also be used to extract the directions of the origin and the X, Y, and Z axes of the coordinate axis in the space polar coordinate system, and scan and extract the map

FIGURE 7: The original image captured by the park camera.

measurement data in the rear-view direction of the aiming point. Due to the different geographical environments, the grooves, bridges, and roads in the measurement process are also different. Careful scanning is required, and part of the data information needs to be verified to measure the target points. According to the method used in this paper, effective measurement can be carried out, and the inspection of the measurement data can be realized after completion. Checking the integrity of the measurement data can ensure the scanning pass rate of each area.

(3) Data processing. The information needs to be preprocessed according to the collected data. This process is more complicated and needs to be preprocessed with the help of RISCANPRO software. According to the data imported from the system and the data in the coordinate system, the GPS can be used for dynamic real-time comparison, and the accuracy of the data can be achieved by multiple verification methods, and the noise with large external interference can be processed and adjusted according to the scanned data.

(4) Extraction of image data features. The database in the RISCANPRO system contains relatively many types of images, but the colors of the images are different, so it is necessary to identify each image separately. In the process of identifying the chart, it is necessary to supplement and explain the data information according to the DXF format file, so as to realize the automatic generation of the panoramic image.

(5) Data integration. Combine the scan information of multiple sites and use the iterative point method for processing. If the deviation is smaller, the result of the data connection is more ideal. Connect more than six pairs of points with the same name to reduce data deviation.

(6) Draw a topographic map. Through the auxiliary operation information of RISCANPRO system, a DXF file is generated, and the CASS system is used to fill in the measured information, and finally a topographic map in the form of DWG is formed.

(7) The accuracy of the analysis data. Because the accuracy of the fully digital stereo 3D reconstruction is flawed, the overlapped range is compared in height when measuring the position and the scan data is automatically generated. The rendering effect shows that the plane position deviation of the fifth point of the scan data is 1.02 m or so, and the deviation of the high-range annotation point is about 0.56 m.

(8) Project summary. This water conservancy project adopts fully digital stereo 3D reconstruction rearview, which greatly improves the measurement speed of this water conservancy project measurement task. Compared with the 3D laser measurement technology, the previous measurement methods are less efficient.

According to the obtained original image, this paper obtains its contour by using the traditional technology and the three-dimensional reconstruction technology in turn, and the comparison result can be shown in Figure 8 in the meantime.

Based on the park image, the eigenvalues of its contour data information are obtained, and different techniques are used to calculate the matching number and matching rate of the obtained park panoramic feature points. The experimental comparison results are shown in Table 1.

According to the test results in Table 1, it can be concluded that using the technology proposed in this paper, the number of park panorama feature matching and matching rate can be obtained, both of which are lower than the 3D reconstruction technology used in this
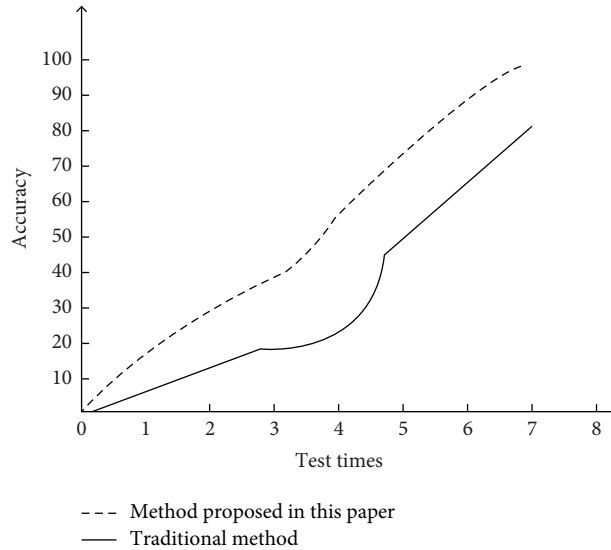
FIGURE 8: Comparison of the results of 3D reconstruction of images under different technologies.

TABLE 1: Number of image feature points and matching rate under different technologies.

Serial number	Traditional technology		Three-dimensional reconstruction technology	
	Number of matching/pieces	Matching rate (%)	Number of matching/pieces	Matching rate (%)
1	630	31.6	630	85.31
2	420	25.7	420	83.71
3	390	23.3	390	90.21
4	320	30.8	320	84.31
5	300	22.5	300	90.61

paper. The feature point matching rate of the three-dimensional reconstruction technology is relatively high, and the accuracy of the corresponding image contour data information is also relatively high.

According to the above experimental results, three-dimensional reconstruction is performed on the acquired images, and the test results are shown in Figure 8.

According to the test and comparison results in Figure 8, it can be seen that the image panoramic image obtained by the 3D reconstruction technique in this paper is more scientific and reasonable. The matching feature points obtained by this technique in the image reconstruction process are more accurate. At the same time, simulation tests can be carried out according to the image matching results. According to the above experimental comparison results, the simulation result diagram as shown in Figure 8 can be obtained, and the results were compared using traditional techniques and 3D reconstruction techniques.

According to the simulation test results in Figure 8, it can be concluded that in the first experimental case, the accuracy of the images that can be generated by the 3D reconstruction technique in this paper is higher than that of the traditional technique, and the accuracy can be improved by 4.6% compared with the traditional algorithm. After two experiments, if the accuracy of the images generated using the 3D

reconstruction technique in this paper will be improved by about 2%. As the number of experiments increases, so does the accuracy of the automatically generated images.

3. Conclusion

In the process of automatic generation of panoramic images by traditional image reconstruction technology, the edge feature data information of the image contour is not completely generated, so that the error value between the image and the actual image is relatively large. Therefore, the fully digital stereo 3D reconstruction method proposed in this paper can effectively improve the accuracy of obtaining the edge feature values of image contours. Finally, the experimental analysis results show that this technical method has high efficiency in the process of matching the feature vectors of panoramic images, and can compare the position features of the image with the feature quantities in the database, and the effect of generating panoramic images is also good, and it has very high use value in the future.

Data Availability

The data used to support the findings of this study are available from the corresponding author upon request.

Conflicts of Interest

The authors declare no conflicts of interest.

Acknowledgments

References

[1] J. Wang and G. Meng, "Application of tilt photogrammetry in surveying and mapping of water conservancy projects," *Bulletin of Surveying and Mapping*, vol. 149, no. 9, pp. 38–52, 2019.

[2] Q. Chen, L. Liu, J. Zhang et al., "Clinical features and prognosis of cervical adenocarcinoma and adenosquamous carcinoma: an analysis of 237 cases," *Electronics Test*, vol. 47, no. 4, pp. 357–361, 2018.

[3] S. Hong and J. Kim, "Three-dimensional visual mapping of underwater ship hull surface using piecewise-planar slam," *International Journal of Control, Automation and Systems*, vol. 18, no. 3, pp. 564–574, 2020.

[4] Y. Piao, L. Xing, M. Zhang, and B. G. Lee, "Three-dimensional reconstruction of far and large objects using synthetic aperture integral imaging," *Optics and Lasers in Engineering*, vol. 107, no. 1, pp. 1–16, 2017.

[5] Z. Gu, J. Chen, and C. Wu, "Three-dimensional reconstruction of welding pool surface by binocular vision," *Chinese Journal of Mechanical Engineering*, vol. 34, no. 1, pp. 47–13, 2021.

[6] C. Y. Chiu, M. Thelwell, T. Senior, S. Choppin, J. HartHart, and J. Wheat, "Comparison of depth cameras for three-dimensional reconstruction in medicine," *Proceedings of the Institution of Mechanical Engineers - Part H: Journal of Engineering in Medicine*, vol. 233, no. 9, pp. 938–947, 2019.

[7] T. Guerneve, K. SubrSubr, Y. Petillot, Petillot, and Yvan, "Three-dimensional reconstruction of underwater objects using wide-aperture imaging sonar," *Journal of Field Robotics*, vol. 35, no. 6, pp. 890–905, 2018.

[8] J. ShiShi and B. ShenShen, "Analysis of thermal effect around an underground storage cavern with a combined three-dimensional indirect boundary element method," *Engineering Analysis with Boundary Elements*, vol. 95, no. 10, pp. 255–265, 2018.

[9] Q. H. Zhang, "Technical method for surveying and mapping of small water conservancy projects," *Surveying and Mapping of Geology and Mineral Resources*, vol. 30, pp. 595–603, 2019.

[10] L. Xin, X. Liu, Z. Yang, X. Zhang, Z. GaoGao, and Z. Liu, "Three-dimensional reconstruction of super-resolved white-light interferograms based on deep learning," *Optics and Lasers in Engineering*, vol. 145, no. 12, Article ID 106663, 2021.

[11] J. Du, X. L. Mao, P. F. Ye, and Q. H. Huang, "Three-dimensional reconstruction and visualization of human enamel ex vivo using high-frequency ultrasound," *Journal of Medical and Biological Engineering*, vol. 37, no. 1, pp. 112–122, 2017.

[12] X. U. Rui and T. W. Luo, "Research on the information extraction of ground three-dimensional laser scanning technology in mountainous area of water conservancy project surveying and mapping," *China Rural Water and Hydropower*, vol. 83, no. 3, pp. 687–696, 2019.

[13] A. Jahanbakhshzadeh, M. Aubertin, and L. Li, "Three-dimensional stress state in inclined backfilled stopes obtained from numerical simulations and new closed-form solution," *Canadian Geotechnical Journal*, vol. 55, no. 6, pp. 810–828, 2018.

[14] W. Tang, H. U. Yulong, Y. E. Ruifeng, and Y. Zhang, "Digital surveying and mapping technology and its application in hydraulic engineering," *Modern Information Technology*, vol. 25, no. 2, pp. 177–187, 2019.

[15] P. F. Yang, "Brief discussion on uav remote sensing application in hydraulic engineering surveying and mapping," *Heilongjiang Hydraulic Science and Technology*, vol. 14, no. 1, pp. 1–7, 2017.

[16] J. Geng, "Technical design and implementation of river and water conservancy project management scope delimitation in jiangsu province," *Geospatial Information*, vol. 233, no. 9, pp. 938–947, 2018.

[17] X. Zheng, "The application of 3d laser scanning technology in water conservancy engineering topographic mapping," *Guangdong Water Resources and Hydropower*, vol. 30, no. 7, pp. 1916–1927, 2017.

[18] X. U. Zhi-Xin, "Application of new surveying and mapping technology in geological survey engineering," *World Nonferrous Metals*, vol. 95, no. 10, pp. 255–265, 2018.

[19] J. X. Fan, "Development and application of digital mapping technology and geological engineering survey," *World Nonferrous Metals*, vol. 30, no. 1, pp. 595–603, 2017.

[20] S. Q. Kou and Z. Shi, "Three-dimensional reconstruction of fracture-split connecting rod joint surface and its strength and stiffness," *Jilin Daxue Xuebao (Gongxueban)/Journal of Jilin University (Engineering and Technology Edition)*, vol. 48, no. 5, pp. 1515–1523, 2018.